Stem cell fate dictated solely by altered nanotube dimension

Seunghan Oh[a], Karla S. Brammer[a], Y. S. Julie Li[b], Dayu Teng[b], Adam J. Engler[b,c], Shu Chien[b,c,1], and Sungho Jin[a,c,1]

Departments of [a]Materials Science and Engineering and [b]Bioengineering, and [c]Institute of Engineering in Medicine, University California at San Diego, La Jolla, CA 92093

Contributed by Shu Chien, December 24, 2008 (sent for review December 4, 2008)

Two important goals in stem cell research are to control the cell proliferation without differentiation and to direct the differentiation into a specific cell lineage when desired. Here, we demonstrate such paths by controlling only the nanotopography of culture substrates. Altering the dimensions of nanotubular-shaped titanium oxide surface structures independently allowed either augmented human mesenchymal stem cell (hMSC) adhesion or a specific differentiation of hMSCs into osteoblasts by using only the geometric cues, absent of osteogenic inducing media. hMSC behavior in response to defined nanotube sizes revealed a very dramatic change in hMSC behavior in a relatively narrow range of nanotube dimensions. Small (≈30-nm diameter) nanotubes promoted adhesion without noticeable differentiation, whereas larger (≈70- to 100-nm diameter) nanotubes elicited a dramatic stem cell elongation (≈10-fold increased), which induced cytoskeletal stress and selective differentiation into osteoblast-like cells, offering a promising nanotechnology-based route for unique orthopedics-related hMSC treatments.

differentiation | mesenchymal | nanotopography | osteogenesis | proliferation

Nanostructures are of particular interest because they have the advantageous feature of a high surface-to-volume ratio, and they elicit a higher degree of biological plasticity compared with conventional micro- or macrostructures. In the field of biomaterial development and in vivo implant technology, the nanoscale structure and morphologenic factor of the surface have played a critical role in accelerating the rate of cell proliferation and enhancing tissue acceptance with a reduced immune response (1, 2). In terms of in vitro cell biology, there has also been much attention placed on cellular responses to their structural surroundings (3). In fact, it has been observed that macro-, micro- and nano-sized topographical factors stimulate behavioral changes in both cells and tissues. Recent studies related to the effect of nanotopography on cellular behavior indicated that osteoblast adhesion and functionality was enhanced by 30% when cultured on a nanograined Al_2O_3 and TiO_2 substrate (4–6) compared with those cultured on a micrograined surface, and nanostructures such as TiO_2 nanotubes with <100-nm spacing showed superior characteristics in bone mineral synthesis (5). However, most of the previous studies on nanostructures and cell responses have mainly used oriented, patterned, or semiordered polymer arrays (7–9) and alumina/polymer hybrid patterned arrays (10).

The material and mechanical characteristics of titanium (Ti) metal, which has a thin native oxide layer of TiO_2, make it an ideal orthopedic material that bonds directly to the adjacent bone surface (11, 12). Fabrication of the nanostructured titanium dioxide (TiO_2) nanotube arrays has been a primary subject of investigation lately because of the wide range of TiO_2 applications in the fields of solar cells (13–16), photocatalysis (17–19), photoelectrolysis (20), sensors (21, 22), and biomaterials (23–25). The presence of a vertically aligned TiO_2 nanotube surface on Ti foils had a critical effect that improved the proliferation and mineralization of osteoblasts (24) and enhanced the mobility, vasodilation, and monolayer formation of endothelial cells (25) because of the unique nanotopographical features and high biocompatibility of the TiO_2 nanotube surface.

Several recent studies have investigated the influence of nanostructures on mesenchymal stem cell (MSC) proliferation and differentiation into specific cell lineages. It is well known that MSCs are multipotent stem cells that can differentiate into stromal lineages such as adipocyte, chondrocyte, fibroblast, myocyte, and osteoblast cell types by generating the appropriate intermediate progenitors for each. By examining the cellular behavior of MSCs cultured in vitro on nanostructures, it can provide some indication and understanding of the effects that the nanostructures may have on the stem cell's response, and possibly how to direct the formation of bone in vivo. Most previous studies have used the combination of osteogenic inducing media having additional chemical factors and nanostructured culture substrates to accelerate osteogenesis and bone formation of MSCs in vitro, but it is difficult to truly distinguish whether the effect of the nanostructured surface topography itself can achieve MSC differentiation without adding chemical factors. Here, we demonstrate that TiO_2 nanotube size can regulate human mesenchymal stem cell (hMSC) differentiation toward an osteoblast lineage in the absence of osteogenic inducing factors and we describe a mechanism for controlling MSC fate based on a narrow range of nanotube dimensions.

Results

We prepared nominally 30-, 50-, 70-, and 100-nm TiO_2 nanotubes on Ti substrates by anodization (25), as depicted in Fig. 1, to determine how the size of the nanotubes would play a role in the cellular response and differentiation of hMSCs [detailed experimental descriptions can be found in *Materials and Methods* and in supporting information (SI) *Materials and Methods*]. The self-assembled TiO_2 nanotube arrays on Ti substrates have a robust and discrete shape, confirmed by SEM images, which show highly ordered nanotubes with 4 different pore sizes between 30 and 100 nm that were created by controlling anodizing potentials (5, 10, 15, and 20 V). Flat Ti substrates (having a native TiO_2 oxidation layer on the surface with analogous chemical composition of the nanostructured TiO_2 substrates) were used as comparison substrata. SEM images of hMSCs cultured on experimental substrata showed that, after 2 and 24 h of incubation, the shape of the hMSCs sitting on top of flat Ti and on various sizes of TiO_2 nanotubes were extremely different (Fig. 2). hMSCs on flat Ti appeared to be more round and stationary; they lacked the noticeable filopodia extensions and cellular propagation fronts like those cultures on TiO_2 nano-

Author contributions: S.O., A.J.E., S.C., and S.J. designed research; S.O. and K.S.B. performed research; A.J.E. contributed new reagents/analytic tools; Y.S.J.L., D.T., S.C., and S.J. analyzed data; and S.O., K.S.B., Y.S.J.L., D.T., S.C., and S.J. wrote the paper.

The authors declare no conflict of interest.

[1]To whom correspondence may be addressed. E-mail: shuchien@ucsd.edu or jin@ucsd.edu.

This article contains supporting information online at www.pnas.org/cgi/content/full/0813200106/DCSupplemental.

© 2009 by The National Academy of Sciences of the USA

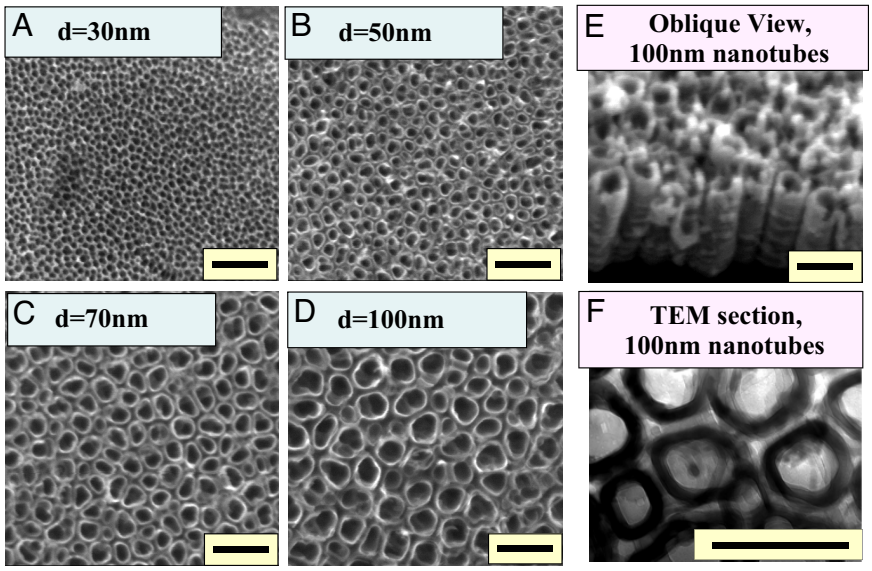

Fig. 1. TiO_2 nanotube. (*A–D*) SEM micrographs (top view) of self-aligned TiO_2 nanotubes with significantly different diameters. The self-assembly layers were generated by anodizing Ti sheets. The images show highly ordered, vertically aligned nanotubes with 4 different nanotube pore diameters, 30, 50, 70, and 100 nm, created by controlling anodizing potentials ranging from 5 to 20 V. (*E*) SEM micrographs (oblique view) of the 100-nm diameter TiO_2 nanotube. (*F*) Cross-sectional transmission electron microscopy (TEM) of the 100-nm diameter TiO_2 nanotubes. (Scale bar, 200 nm.)

tubes. However, on nanotube surfaces especially for the cases of larger-diameter nanotubes, a large number of prominent filopodia and unidirectional lamellipodia extensions were apparent on the nanotube structures even after just 2 h of culture (Fig. 2 *Upper*). This trend becomes much more apparent if the hMSC culture time is extended to 24 h (Fig. 2 *Lower*), and significantly more pronounced when the nanotube diameter is increased (lamellipodia are shown by the yellow arrows). As indicated by the red arrows, hMSCs exhibit cellular morphologies with extraordinary elongation of as much as 200 μm in length on 100-nm TiO_2 nanotube surfaces. This is $\approx$10-fold increase in the hMSCs cellular elongation length compared with the identical culture conditions for the 30-nm nanotubes.

Higher magnification SEM images of TiO_2 nanotube substrata (Fig. 3) after 2 h of culture reveal the adhesion of many round protein aggregates, $\approx$30 nm in diameter, deposited from serum in the culture media. These protein aggregates are most likely settling on the surface, acting as a preexisting, accessible protein coating, which would have implications on how the cells initially perceive the surface and the way they attach. Protein aggregates are rather quickly deposited after only 2 h of incubation on the wall top of the nanotubes. Less protein aggregate deposition, with a sparse distribution, is observed on flat Ti samples, whereas aggregate coating of the Ti nanotubes directly scales with nanotube diameter.

The cell adhesion and elongation aspects were further studied to elucidate the nanotube size dependence of hMSC behavior.

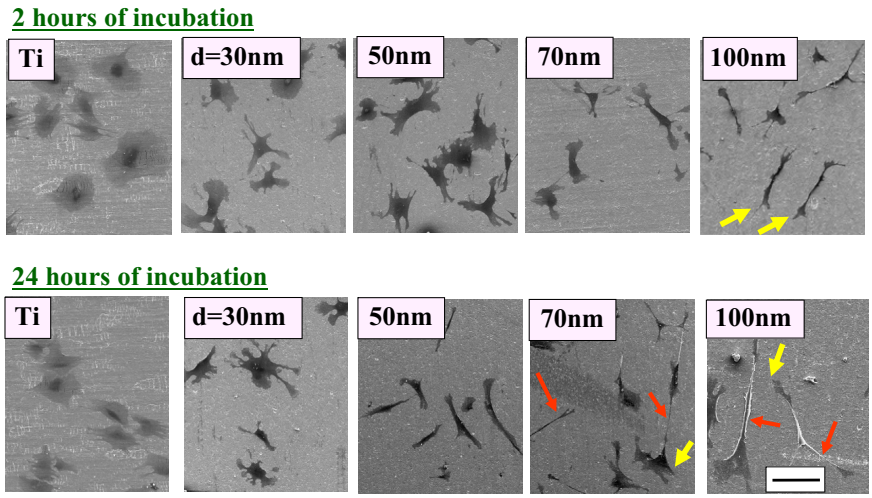

Fig. 2. SEM micrographs of human mesenchymal stem cells (hMSCs) on flat Ti and 30-, 50, 70-, and 100-nm diameter TiO_2 nanotube surfaces after 2 h of culture. (Scale bar, 100 μm.) Cells are flat, spread out, and round-shaped on the flat Ti substrate, they are somewhat flat and rounded on 30-nm nanotubes, and they become progressively elongated as the nanotube diameter is increased to 50-nm diameter and beyond. Extraordinary cell elongation is induced on nanotubes with diameters of 70 and 100 nm (see red arrows), especially after the 24 h culture. More mobile morphologies are indicated by the presence of somewhat elongated leading edges of lamellipodia (yellow arrows) seen on 70 and 100 nm nanotubular surfaces. The cell shapes suggest that cells are more elongated on the bigger TiO_2 nanotubes.

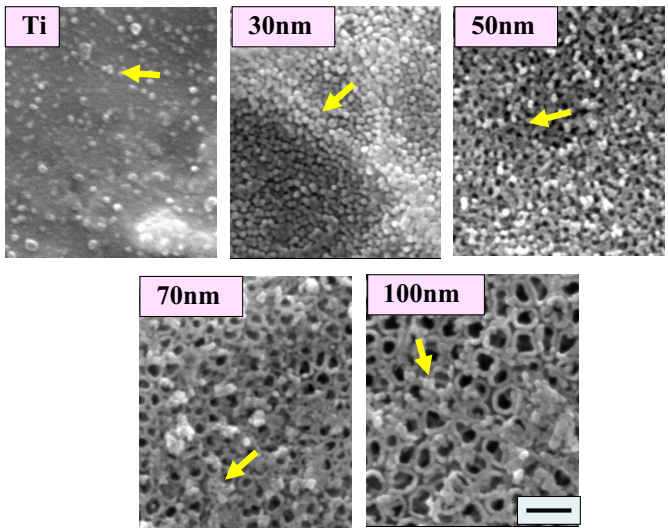

Fig. 3. SEM micrographs showing extracellular matrix aggregates on the surfaces of flat Ti and 30-, 50-, 70-, and 100-nm diameter TiO_2 nanotubes after 2 h of hMSC culture. (Scale bar, 200 nm.) Note that the presence of protein aggregates is infrequent on Ti, abundant on 300-nm nanotubes, and much less on the larger-diameter 70- and 100-nm nanotubes.

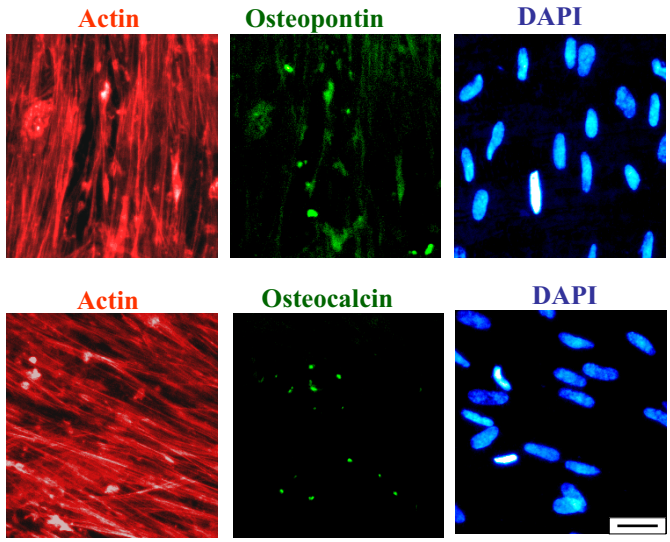

Fig. 4. Immunofluorescent images of OPN (*Upper Center*) and OCN (*Lower Center*), as well as actin (*Left*) and DAPI (*Right*), on 100-nm diameter TiO_2 nanotubes after 3 weeks of culture. (Scale bar, 50 μm.)

As shown in Fig. S1*a*, it became apparent that the number of adhered hMSCs on the experimental substrata decreased almost inversely proportional to the pore size of the TiO_2 nanotubes at the critical early stage of hMSC interaction with substrata (within the initial 24 h of incubation time). After prolonged incubation, cell growth for all other substrates caught up and these differences eventually were not as apparent because of the confluency of the cells, as might be anticipated at 7 days of culture time.

To understand the relationship between the nanodimensional cues and hMSC cell behavior, we also carried out a quantitative analysis of cellular morphological elongation. As shown in Fig. S1*b*, the elongation ratio of hMSCs increased with increasing size of TiO_2 nanotubes. The largest TiO_2 nanotubes showed an average elongation ratio of length/width as large as $\approx$10, whereas the small-diameter nanotubes of 30 nm (as well as the flat Ti) exhibited a basically isotropic configuration with an overall average elongation ratio of more or less $\approx$1. These cell elongation results were also confirmed with live cell imaging by using fluorescein diacetate (FDA) staining, which is shown in Fig. S2. The extraordinary stretching of hMSCs for the larger-diameter nanotubes of 70 and 100 nm is evident from the figure and demonstrate that cell elongation and adhesion appear to be inversely related to one another on Ti nanotubes.

The elongation/stretching of the hMSCs on larger-diameter nanotubes resulted in a preferential differentiation into osteogenic lineage, which was confirmed by immunofluorescent staining of 2 common protein osteogenetic markers: osteopontin (OPN) and osteocalcin (OCN). This analysis for the detection of osteogenic protein expression of hMSCs was conducted on cells cultured for 21 days. The immunofluorescent results, which are given in Fig. 4 for 100-nm TiO_2 nanotubes, showed that hMSCs had recognizable OCN- and OPN-positive staining with staining shapes associated with osetoblast cells, whereas hMSCs on the much smaller-diameter nanotubes and flat Ti substrata did not elicit any positive staining. Fig. 4 *Upper* represents osteopontin (OPN) staining (together with actin and dapi staining for the same image area to also illustrate the cytoplasmic actin skeleton and cell nuclei), whereas Fig. 4 *Lower* shows the osteocalcin (OCN) staining (again with actin and dapi staining of the same image area).

To further support the immunofluorescent staining results described above, osteoblast gene expression (OCN, osteocalcin; OPN, osteopontin; and ALP, alkaline phosphatase) was also studied by quantitative real-time PCR analysis after 14 days of incubation, with the analysis data shown in Fig. 5. hMSCs on 70- and 100-nm TiO_2 nanotubes demonstrated various levels of osteogenic up-regulation and showed a significantly higher level of expression than those on other substrata ($P < 0.01$). The 100-nm nanotubes displayed the highest up-regulation of all selected osteoblastic genes among the experimental groups at just 14 days of incubation and were closest to chemically induced osteoblast gene expression (positive control). Together, immunofluorescence and real-time PCR results seemed to confirm that 100-nm nanotubes have the potential as a guided differentiation tool for directing hMSCs into osteoblast-like cells in the absence of osteogenesis-inducing media. In contrast, the 30-nm nanotube sample exhibited a significantly lower degree of almost negligible osteoblast gene expression (considering the magnitude of error bars), as indicated in Fig. 5.

Discussion

Serum is widely used in the culturing of eukaryotic cells and it is known to contain many extracellular matrix globular proteins

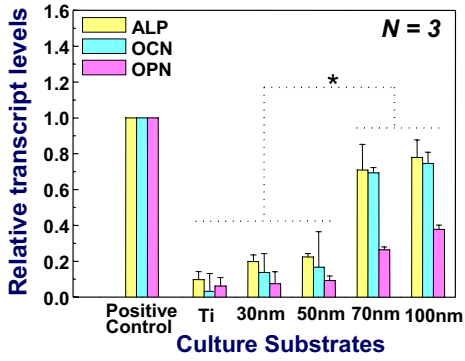

Fig. 5. Quantitative PCR analysis for ALP, OCN, and OPN. Plastic cell culture plate with osteogenic inducing media was used as a positive control for osteogenic differentiation. *, Significant differences between Ti, 30- and 50-nm nanotubes vs. 70- and 100-nm nanotubes for ALP, OCN, and OPN gene expressions ($P < 0.01$).

and glycoproteins as major components. Immunofluorescent staining for 2 serum proteins, BSA and fibronectin, on the sample surfaces after 2 h of incubation in media revealed positive results for both proteins. Fibronectin was detected on the surfaces (Fig. S3) as well as albumin. Fibronectin, which is known to play a major role in cell adhesion, is a high-molecular-weight glycoprotein, which when in solution coils up into a nanometer-sized aggregate. The size of albumin is well known to also be several nanometers, which may have been agglomerated/conformed in the ≈30- to 60-nm size on top of the sample surfaces during the ≈2 h of incubation time. Although further studies are needed to identify the detailed nature of the protein attached to the nanotube surface, we clearly demonstrate that there is a significant dependence of protein attachment on nanotube absent of any chemical stimulus. The serum in our experimentation is identical to that used by Dalby *et al.* (7).

It is reasonable that the control surface, i.e., flat Ti (with a TiO_2 native oxide layer), has a lower population of these protein aggregates, because it is less hydrophilic than the higher-surface-area TiO_2 nanotube surfaces, in general, based on water droplet contact angle measurements. It would be interesting to perform additional studies on the effect of hydrophilicity of TiO_2 nanotubes on cell and protein adhesion and growth. From the nanoscale perspective, the nanotubes are generally of uniform height and diameter, although there are slight variations. On microscopic scales, however, there could be some local nonuniform heights due to the surface roughness of the starting material and various process steps, such as substrate anodization, addition of serum-containing media, and associated protein (i.e., fibronectin) adsorption. Atomic force microscopy analyses indicate that the variations in the processed sample surface height >20-μm scan are $<\approx$200 nm, which may be viewed as being insignificant from the context of what a cell sees. Because sharp edges are known to create spots of high surface energy to facilitate focal adhesion, further studies are needed to clarify how much, if any, such nonuniformity in nanostructure affects the hMSC adhesion to TiO_2 nanotube substrates.

Among the various sizes of TiO_2 nanotubes, the smaller-dimension nanotubes of 30-nm diameter, and to some extent for the 50-nm TiO_2 nanotubes, showed a much higher population of protein aggregates on the top surface when compared with nanotubes with 70-nm or 100-nm diameter. The 30-nm diameter nanotubes, in particular, elicit complete substrate surface coverage with the protein aggregates. The reason for the much reduced protein aggregate adsorption observed on the top of larger-diameter nanotubes of 70- and 100-nm diameter is most likely because ≈30-nm size protein aggregates are just too small to anchor on 70- or 100-nm diameter nanopores with much larger open pore spaces, because the protein aggregates initially attach only to the available surfaces that are the top portion of the nanotube walls. We believe that we have found a threshold point of nanotube size (≤50 nm) where the adhesion of proteins (≈30-nm-size regime) initially determines the degree of cell adhesion, a critical observation in this study. The phenomenon of initial protein adsorption is very important in understanding why hMSCs were more elongated on the 100-nm nanotube surface than hMSCs on the smaller-sized nanotube surfaces. Extracellular matrix (ECM) proteins are required for a cell to adhere to the surface and to be able to spread out. Within an initial incubation time (say, <6 h), the proteins available in the culture media from the serum adsorb to the surface and act as the preliminary ECM, which can help cell adhesion considerably at the earliest stages of culture before cells begin secreting their own ECM. hMSCs cultured on <50-nm TiO_2 nanotubes can more easily attach to the surface because of the high population of ECM proteins deposited across the entire surface as indicated in Fig. 3. However, hMSCs cultured on 100-nm TiO_2 nanotubes probably would have to struggle to search for areas where more protein aggregates have been deposited to establish initial contact because there is much more interprotein aggregate spacing due to the large pore sizes in the nanostructure. Eventually, the hMSCs have to extend their filopodia extensions excessively and move to find proteins, thus becoming more mobile and forming more extraordinarily elongated shapes.

For further understanding of the hMSC elongation behavior and related effect on stem cell differentiation, 2 possible routes of systematic investigations could be used in the future to force the hMSCs to elongate into specific commanded dimension. These include (*i*) dictating the substrate dimensional cues with selected line pattern width for control of hMSC cell width and elongation (for example, by using hMSC adherent line region separated by hMSC-repelling regions such as coated with polyacrylamide gel), and (*ii*) dictating the distance that the hMSCs need to travel and stretch by using the intentionally spaced extracellular islands [for example, by providing a periodically placed ECM island array pattern (e.g., in a triangular array configuration by nanoimprint stamping transfer)] that would dictate how much the hMSCs have to stretch out to reach the next available ECM island(s). Such experiments can further elucidate the effect of artificially controllable geometrical cues on stem cell enrichment or differentiation, and may provide valuable bioengineering methodologies for stem cell control and beneficial therapeutic applications.

It is notable that the hMSCs adhered to the smallest dimensioned 30-nm nanotubes more efficiently in the first 2 h probably because of the high protein population initially on the surface (Fig. S1*a*). Also noticeable in the figure is that the highest quantity of adhered and growing hMSC cells was maintained on the 30-nm nanotube substrates after the first 24 h of incubation. However, in comparison, as indicated in the SEM micrographs and FDA images, the larger-diameter nanotubes (70- and 100-nm diameter) that induced a dramatic cell elongation increased osteogenic expressions (Figs. 4 and 5) with a lower amount of adhered cells.

We have described in previous studies (24) that the long-range structure of TiO_2 nanotubes is neither patterned nor highly ordered, but they do have a robust and discrete nanotube shape. Dalby *et al.* (7) reported that MSC cultured on highly ordered poly(methylmethacrylate) (PMMA) nanopatterns showed negligible osteogenic differentiation, but randomized PMMA nanotopography demonstrated MSC osteoblastic morphologies after 21 days of incubation with cell growth media. We have similarly demonstrated, with our nonordered TiO_2 nanotube arrays, results that are in agreement with their findings where hMSC osteogenic differentiation is observed without osteogenic inducing media. However, we demonstrate in this report a clear mechanism for MSC fate based on the TiO_2 nanotube geometry providing an explanation for control of MSCs by specific nanotube dimensions.

This observed attainment of differentiation in the absence of additional biochemical inducing agents is critical to the success of our nanotopography-induced differentiation shown in the following results. Many biochemists and molecular biologists induce differentiation by chemical factors in vitro, but there is no well-understood way of controlling such factors and precise concentrations in vivo. In fact, the side effects of many chemicals such as dexamethasone or β-glycerophosphate, typical osteogenic inducing reagents, are not known because the body does not encounter these types of chemicals naturally. In contrast, our approach relies on controlling stem cell fate by using only the nanotopography, which is much more dependable, and we can expect a similar and more reproducible in vivo response because we do not have the in vivo variability and side effects associated with chemical additions.

In terms of the correlation between initial cell density and differentiation of mesenchymal stem cells, Pittenger *et al.* (27)

and McBeath *et al.* (28) reported that initial cell-plating density made critical effects on the differentiation of mesenchymal stem cells, and a lower cell density showed better osteoblastic differentiation compared with a higher cell density in the presence of osteogenic inducing media. From our results we have shown that 100-nm nanotubes elicited a lower initial cell number (Fig. S1*a*), but a higher osteogenic gene expression than other sizes of nanotubes (Fig. 5). Although the final cell density eventually saturates after a longer incubation and becomes essentially the same for different diameter nanotubes, it is likely that the initial cell density has a lasting impact on the eventual stem cell fate. From this point of view, we too show a correlation between cell density and differentiation and can draw some similarity between Pittenger *et al.* and McBeath *et al.*'s observations (27, 28) and our findings.

Furthermore, our experimental results indicated that the hMSCs were extraordinarily more stretched and probably stressed on the 100-nm nanotubes, ≈10 times longer in average cell length than those on the 30-nm nanotubes as shown in the SEM micrographs of Fig. 2. It is most probable that this elongated morphology causes cellular cytoskeletal tension and stress on the hMSCs cultured on 70- to 100-nm diameter regime nanotubes compared with a normal cell culture condition on a flat surface substrate. It is well known that various kinds of physical stresses from the substrate morphology and topography can accelerate stem cell differentiation into a specific cell lineage (29–35); our data show a similar scenario.

In addition, the SEM and FDA images of hMSCs on all sizes of TiO_2 nanotubes showed the formation of more filopodia, lamellipodia, and cellular extensions compared with those on flat Ti. Our results are also in general agreement with other studies relating cellular extensions and differentiation (7, 8).

The trends of hMSC adhesion, elongation, and differentiation behavior reported here as a function of nanotube dimension seem to reveal a specific mechanism that determines the stem cell fate solely on the geometric cues of the surface. The mechanism follows that, on small-diameter nanotubes, increased cell adhesion and growth with minimal differentiation seem to be prevalent, because this is in part due to the protein aggregate adhesion configurations induced by the small nanotubes. On larger-diameter nanotubes, hMSC cells are forced to elongate and stretch to search for protein aggregates, and as a result, are forced/guided to differentiate specifically into osteoblast cells. This claim is based on the well-established research that shows when stem cells are stressed due to the high elastic modulus, for example, stiff substrates; differentiation into osteoblast cells is enhanced (7, 8, 32). From the results of our research, we have developed a concept of stem cell fate based on nanotube dimension and it is schematically illustrated in Fig. 6, with the protein aggregate dimensions and hMSC elongation trends also incorporated. This suggested mechanism is, in a sense, in agreement with the general notion that when cells are busy adhering and growing, their functionality is expected to be reduced, and when the stem cells are stressed, they tend to differentiate into a specific lineage to accommodate the stress.

Although the hMSC growth and differentiation behavior appear to be somewhat saturating at ≈100-nm diameter, it would nevertheless be interesting to investigate their behavior on larger-diameter TiO_2 nanotubes so as to find an ultimate saturation limit of stem cell differentiation. However, it is noted that such larger-diameter TiO_2 nanotubes beyond the ≈100 nm regime are currently difficult to fabricate by the same self-assembly anodization processing techniques used here, and hence new process approaches are needed to enable such a study.

This research elucidates the effects of the nanotopography of TiO_2 nanotubes on mesenchymal cell adhesion, morphology, and osteogenic differentiation, all in the absence of osteogenic media. We have made a striking discovery that the cell adhesion and growth (without differentiation) vs. guided differentiation is strongly correlated with the size of nanotubes in a relatively small window of nanotube diameter ranges. We also demonstrate that a guided osteogenic differentiation of hMSCs can be controllably manipulated by selective sizing of the nanotube dimensions. Because the TiO_2 nanotubes are excellent osseointegration biomaterials as evidenced by in vitro data (24), and our preliminary in vivo animal data indicating a strong new bone integration on the nanotube surface with reduced soft tissue trapping (data not shown), the nanotube surface can perform dual therapeutic functions of specifically guided differentiation and strong osseointegration for new bone formation. We forecast that these results can be a milestone for the further study of stem cell control and implant development, in terms of its application as a therapeutic platform as well.

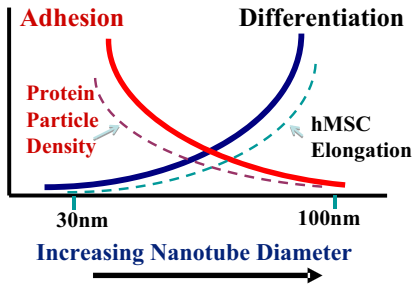

Fig. 6. Schematic illustration of the overall trends of nano cue effects on hMSC fate and morphology after a 24-h culture. The change in hMSC cell adhesion and growth without differentiation (solid red line) has the same trend as protein particle density (broken red line), whereas that of differentiation (solid blue line) has the same trend as hMSC elongation (broken blue line).

Materials and Methods

TiO_2 Nanotube Fabrication. The protocol for preparation of TiO_2 nanotubes by anodization process for cell culture is similar to what we used (5, 24, 25) and is described as follows. The nanotubes were formed on a Ti sheet (Alfa-Aesar; 0.25 mm thick, 99.5%) by using a mixture of 0.5 wt % hydrofluoric acid (EM Science; 48%) and acetic acid (Fisher; 98%, volumetric ratio = 7:1) at 5, 10, 15, and 20 V for 30 min to obtain different diameter nanotubes. A platinum electrode (Alfa-Aesar; 99.9%) served as the cathode. The specimen was rinsed by deionized water, dried at 80 °C, and heat treated at 500 °C for 2 h to transform the as-anodized amorphous TiO_2 nanotubes into crystalline phase. The specimens (1.27 × 1.27 cm^2 area) used for all experiments were sterilized by autoclaving before use. An identically sized flat Ti sample was used as a control after being chemically cleaned by acetone and isopropyl alcohol, dried, and autoclaved.

Cell Culture. Human mesenchymal stem cells (hMSCs) were obtained from Lonza Corporation. The cell growth media were composed of α-MEM (Invitrogen), 10% Fetal Calf Serum (FCS) (Invitrogen), 100 units/mL penicillin, and 100 μg/mL streptomycin (Invitrogen). For preparing positive control in this research, osteogenic inducing media were also prepared by adding 10 nM dexamethasone (Sigma), 150 μg/mL L-ascorbic acid (Sigma), and 10 mM β-glycerophosphate (Calbiochem) to cell growth media. The cells were cultured in a 5% CO_2 incubator at 37 °C. All experiments of hMSCs were conducted with cultures at passage 4.

Scanning Electron Microscopy (SEM) for Substrate and Cell Morphological Examination. Initially cells were plated on the substrates at a density of 1×10^4 cells per mL. After 2 h of culture, the cells on the substrates were washed with 1× PBS and fixed with 2.5% glutaraldehyde in 0.1× PBS for 1 h. After fixation, they were washed 3 times with 1× PBS for 10 min each wash. Then the cells were dehydrated in a graded series of ethanol (50, 70, 90, and 100%) for 30 min each and left in 100% ethanol until they were dried by supercritical point CO_2. Next, the dried samples were sputter-coated with very thin gold for SEM examination. The morphology of the TiO_2 nanotubes, as well as that of the adhered cells, was observed by using SEM (XL30, FEI Corporation).

Immunofluorescence of Actin and Osteopontin/Osteocalcin. After 3 weeks of culture, the cells on the Ti and TiO_2 nanotube substrates were fixed in 4% paraformaldehyde in 1× PBS for 15 min at room temperature. Once fixed, the cells were washed twice with 1× wash buffer (1× PBS containing 0.05% Tween-20). To permeablilize the cells 0.1% Triton X-100 in 1× PBS solution was added for 10 min. The cells were washed twice with wash buffer. Then the samples were incubated for 1 h at room temperature in 1% BSA/1× PBS followed by the addition of antiosteopontin (OPN) antibody (1:100, AKm2A1, Santa Cruz Biotechnology)/antiosteocalcin (OCN) antibody (1:100, OC4–30, QED Bioscience), and incubated for overnight at 4 °C. After incubation, cells were washed 3 times for 5 min each wash with 1× wash buffer. Goat anti-mouse IgG-FITC (1:100, Santa Cruz Biotechnology) and TRITC-conjugated phalloidin (1:40, Invitrogen) in 1× PBS was added for double staining and the cells were incubated again for 1 h at room temperature. The cells were washed 3 times with 1× wash buffer for 5 min each wash. Then, the samples were stained by DAPI (1:1000, Chemicon) for nucleus staining. The samples were then inverted onto coverslips mounted, visualized, and photographed by an epifluorescence microscope (DM IRB, Leica Microsystems).

Real-Time PCR. After 2 weeks of culture, total RNA of the cells on the Ti and TiO_2 nanotube substrates were extracted with TRIzol (Sigma), and reverse-transcribed into cDNA by qScript cDNA Synthesis Kit (Quanta BioSciences). Real-time PCR was performed by Taqman Gene Expression Assays (Applied Biosystems), and the information of Taqman PCR primer is as follows: GAPDH (Hs99999905_m1; Amplicon length, 122), ALP (Hs01029141_g1; Amplicon length, 71), OCN (Hs00609452_g1; Amplicon length, 74) and OPN (Hs00960942_m1; Amplicon length, 63). Real-time PCR was carried out by using Taqman Fast Universal PCR Master Mix and 7900 HT Fast Real-Time PCR System (Applied Biosystems). cDNA samples (1 μL for total volume of 20 μL) were analyzed for gene of interest and for house-keeping gene GAPDH. The comparison test of cycle-threshold point was used to quantify the gene expression level of each sample. In this study, all levels of expression were normalized by the level of expression of positive control (hMSCs cultured with osteogenic inducing media).

Statistical Analysis. In terms of cell count, cell elongation, and real-time PCR assay, all data were expressed as mean ± standard error, and analyzed statistically by the paired Student's *t* test method. Significant difference was determined at P values at least <0.01.

ACKNOWLEDGMENTS. We thank S. Chirasatitsin for assistance in atomic force microscopy analysis. The hMSC experiments were carried out at Human Stem Cell Core Facility at University of California at San Diego. This work was supported in part by California Institute for Regenerative Medicine (CIRM) Postdoctoral Fellowship (S.O.) and Seed Grant RS1-00172–1-(to S.C.), National Institutes of Health Grant HL-080518 (to S.C.), and the Iwama Endowed Fund at University of California at San Diego (S.J.).

1. Jung DR, *et al.* (2001) Topographical and physicochemical modification of material surface to enable patterning of living cells. *Crit Rev Biotechnol* 21(2):111–154.
2. Mahdavi A, *et al.* (2008) A biodegradable and biocompatible gecko-inspired tissue adhesive. *Proc Natl Acad Sci USA* 105:2307–2312.
3. Curtis AS, Varde M (1964) Control of cell behavior: Topological factors. *J Natl Cancer Inst* 33:15–26.
4. Webster TJ, Ergun C, Doremus RH, Siegel RW, Bizios R (2000) Enhanced functions of osteoblasts on nanophase ceramics. *Biomaterials* 21(17):1803–1810.
5. Oh SH, Finones RR, Daraio C, Chen LH, Jin S (2005) Growth of nano-scale hydroxyapatite using chemically treated titanium oxide nanotubes. *Biomaterials* 26(24):4938–4943.
6. Popat KC, *et al.* (2006) Osteogenic differentiation of marrow stromal cells cultured on nanoporous alumina surfaces. *J Biomed Mater Res A* 80(4):955–964.
7. Dalby MJ, *et al.* (2007) The control of human mesenchymal cell differentiation using nanoscale symmetry and disorder. *Nat Mater* 6(12):997–1003.
8. Dalby MJ, *et al.* (2006) Osteoprogenitor response to semi-ordered and random nanotopographies. *Biomaterials* 27(15):2980–2987.
9. Ruiz SA, Chen CS (2008) Emergence of patterned stem cell differentiation within multicellular structures. *Stem Cells* 26(11):2921–2927.
10. La Flamme KE, *et al.* (2007) Biocompatibility of nanoporous alumina membranes for immunoisolation. *Biomaterials* 28(16):2638–2645.
11. Linder L, Carlsson A, Marsal L, Bjursten LM, Branemark PI (1988) Clinical aspects of osseointegration in joint replacement. *J Bone Joint Surg* 70(B):550–555.
12. Puleo DA, Holleran LA, Doremus RH, Bizios R (1991) Osteoblast response to orthopedic implant materials in vivo. *J Biomed Mater Res A* 25:711–723.
13. Mor GK, Varghese OK, Paulose M, Shankar K, Grimes CA (2006) A review of highly ordered, vertically oriented TiO2 nanotube arrays: Fabrication, material properties, and solar energy applications. *Solar Energy Mater Solar Cells* 90:2011–2075.
14. Zhu K, Neale NR, Miedaner A, Frank AJ (2007) Enhanced charge-collection efficiencies and light scattering in dye-sensitized solar cells using oriented TiO2 nanotubes arrays. *Nano Lett* 7(1):69–74.
15. Shankar K, Mor GK, Prakasam HE, Varghese OK, Grimes CA (2007) Self-assembled hybrid polymer-TiO2 nanotube array heterojunction solar cells. *Langmuir* 23(24):12445–12449.
16. Kislyuk VV, Dimitriev OP (2008) Nanorods and nanotubes for solar cells. *J Nanosci Nanotechnol* 8(1):131–148.
17. Albu SP, Ghicov A, Macak JM, Hahn R, Schmuki P (2007) Self-organized, free-standing TiO2 nanotube membrane for flow-through photocatalytic applications. *Nano Lett* 7(5):1286–1289.
18. Jia Y, *et al.* (2007) Synthesis and characterization of TiO2 nanotube/hydroquinone hybrid structure. *J Nanosci Nanotechnol* 7(2):458–462.
19. Su H, Dong Q, Han J, Zhang D, Guo Q (2008) Biogenic synthesis and photocatalysis of Pd-PdO nanoclusters reinforced hierarchical TiO2 films with interwoven and tubular conformations. *Biomacromolecules* 9(2):499–504.
20. Paulose M, *et al.* (2006) Anodic growth of highly ordered TiO2 nanotube arrays to 134 microm in length. *J Phys Chem B* 110(33):16179–16184.
21. Liu S, Chen A (2005) Coadsorption of horseradish peroxidase with thionine on TiO2 nanotubes for biosensing. *Langmuir* 21(18):8409–8413.
22. Varghese OK, Grimes CA (2003) Metal oxide nanoarchitectures for environmental sensing. *J Nanosci Nanotechnol* 3(4):277–293.
23. Park J, Bauer S, von der Mark K, Schmuki P (2007) Nanosize and vitality: TiO2 nanotube diameter directs cell fate. *Nano Lett* 7(6):1686–1691.
24. Oh S, *et al.* (2006) Significantly accelerated osteoblast cell growth on aligned TiO2 nanotubes. *J Biomed Mater Res A* 78(1):97–103.
25. Brammer KS, Oh S, Gallagher JO, Jin S (2008) Enhanced cellular mobility guided by TiO2 nanotube surfaces. *Nano Lett* 8(3):786–793.
26. Aguirre KM, McCormick RJ, Schwarzbauer JE (1994) Fibronectin self-association is mediated by complementary sites within the amino-terminal one-third of the molecule. *J Biol Chem* 269:27863–27868.
27. Pittenger MF, *et al.* (1999) Multilineage potential of adult human mesenchymal stem cells. *Science* 284(5411):143–147.
28. McBeath R, Pirone DM, Nelson CM, Bhadriraju K, Chen CS (2004) Cell shape, cytoskeletal tension, and RhoA regulate stem cell lineage commitment. *Dev Cell* 6(4):483–495.
29. Yamamoto K, *et al.* (2005) Fluid shear stress induces differentiation of Flk-1-positive embryonic stem cells into vascular endothelial cells in vitro. *Am J Physiol* 288(4):H1915–H1924.
30. Saretzki G, *et al.* (2008) Downregulation of multiple stress defense mechanisms during differentiation of human embryonic stem cells. *Stem Cells* 26(2):455–464.
31. Altman GH, *et al.* (2002) Cell differentiation by mechanical stress. *FASEB J* 16(2):270–272.
32. Engler AJ, Sen S, Sweeney HL, Discher DE (2006) Matrix elasticity directs stem cell lineage specification. *Cell* 126:677–689.
33. Norgaard R, Kassem M, Rattan SI (2006) Heat shock-induced enhancement of osteoblastic differentiation of hTERT-immortalized mesenchymal stem cells. *Ann N Y Acad Sci* 1067:443–447.
34. Benoit DS, Durney AR, Anseth KS (2007) The effect of heparin-functionalized PEG hydrogels on three-dimensional human mesenchymal stem cell osteogenic differentiation. *Biomaterials* 28(1):66–77.
35. Mirmalek-Sani SH, *et al.* (2006) Characterization and multipotentiality of human fetal femur-derived cells: Implications for skeletal tissue regeneration. *Stem Cells* 24(4):1042–1053.